Studies of Crosstalk on the MINOS' Hamamatsu M64 Photomultipliers

Anatael Cabrera
University of Oxford

NuMI Note 976

December 19, 2003

Abstract

This note describes the studies accomplished at Oxford to understand the crosstalk in the R5900-00-M64 (M64) photomultipliers. A sample of 9 photomultipliers was used to identify and measure crosstalk in the M64s for this analysis. Two components of crosstalk were found. The first component causes a drift toward positive charge values of the whole charge distribution of the cross-talked pixels. The second component is characterised by drawing photo-electron peaks in the charge distribution of the cross-talked pixels. The pattern of both components is described such that crosstalk can be inserted into the MINOS simulation packages for further studies of crosstalk on the performance of the MINOS detectors.

1 Crosstalk in the MINOS Detectors

The MINOS Near detector uses M64[1] multi-anode photomultipliers (PMT) to read out the scintillation light coming from MINOS calorimeter[2]. Because of the multi-anode structure of M64s, they are very likely to suffer from crosstalk. Crosstalk in the M64 is identified by encountering some charge in non-illuminated pixels. An average of about 10% total crosstalk has been measured in M64s in previous measurements[3].

Crosstalk is quantified as the fractional charge cross-talked ($Q_{non-injected(j)}$) to the injected charge ($Q_{injected(i)}$), as shown in Eq.1.

$$X_{j,i} = \frac{Q_{non-injected(j)}}{Q_{injected(i)}} \tag{1}$$

Crosstalk may sizably affect calorimetry, reconstruction, de-multiplexing (in the Far detector) and calibration procedures at MINOS. Therefore, the understanding of crosstalk pattern and magnitudes may be of capital importance to MINOS. In addition, crosstalk must be well understood in order to fully simulate the response of all the MINOS detectors. In this note, we describe our measurements of crosstalk

and provide feasible avenues to parametrise its pattern such that it can be readily include into MINOS simulation packages.

The Oxford MINOS group built a test stand to quantify general characteristics of all the MINOS M64s. Part of our standard data acquisition procedure includes dedicated crosstalk runs. Crosstalk runs are taken by injecting light 10,000 times in each pixel, while recording the charge in all 64 anodes. All the anode charges are stored into ROOT TTrees for off-line analysis. Prior to any crosstalk run, a pedestal run was taken to allow pedestal subtraction.

In these studies we intend to understand the general trends of crosstalk in M64s based on a sample of 9 good[1] M64s. Only one light level was used for these studies. The experimental setup, DAQ description together with the extension of the method hereby described to all the MINOS' M64s at different light levels can be found in [4].

2 M64 Crosstalk Components

The charge distribution of a non-injected pixel should exhibit the pedestal peak whose mean should be zero ADC counts after pedestal subtraction. When light is injected in one of the pixel some distortion is produced in the charge distribution of some of the non-illuminated pixels. This kind of distortion is caused by crosstalk. An example of how a non-illuminated cross-talked pixel charge distribution looks like is shown in Fig.1. Two major changes has been triggered by the crosstalk. First, the pedestal peak (and the whole distribution) has been shifted slightly toward positive charge values. We shall associate this effect to *"Electrical Crosstalk"* (EXT). Second, the charge distribution exhibits the occurrence of photo-electron (PE) peaks, whose mean is approximately 190ADC counts with the RABBIT electronics sensitivity. This second component shall be associated to *"Optical Crosstalk"* (OXT). The crosstalk in the M64 appears to be fully characterised by these two crosstalk components: OXT and EXT. A cartoon of the crosstalk in the M64 is illustrated in Fig.3.

In order to characterise each of the crosstalk components, a cut had to be developed to separate them. Fig. 2 shows the correlation between one of the 63 non-illuminated pixels charge distributions and the illuminated pixel charge distribution. Since such a correlation may have crucial information about EXT, we developed a 2D-cut to separate the two crosstalk components for each non-illuminated charge distribution pixel.

The following steps were performed to make sure that the correlation information remain:

1. Make a coarse separation of the between EXT and OXT in 1D - red line in Fig. 1.

2. Fit a straight line to the profile histogram of the EXT (OXT removed). The fit should reflect information of the correlation, as indicated by the red line in Fig. 2.

[1] *Good* meaning that met all the conditions agreed with Hamamatsu for MINOS to accept the PMT.

3. The 2D-cut was defined by a parallel straight line to the red line with a further shift by 2.5σs of the pedestal width toward positive charge values. This is illustrated by the green line in Fig. 2.

The green line in Fig. 2 defines what we defined as the boundary between EXT (below) and OXT (above): the 2D cut. Once the two components were successfully separated, the number of entries, MEANs and RMSs of each distribution were used to characterise each crosstalk component.

3 Electrical Crosstalk

This component is responsible for the shift of the pedestal peak toward positive charge values. This kind of crosstalk is characterised for happening very often but drawing little charge: always less than 1PE.

EXT showed a strong dependence upon the distance between the cross-talked pixel and the illuminated pixel, as shown in Fig.4. The shape of this structure together its independence upon cuts on neighbouring readout electronics channels, proved that the pattern belonged to the PMTs having very negligible effect from the also found electronics crosstalk.

Our hypothesis for the mechanism behind this type of crosstalk is the leakage of secondary electrons from the illuminated cell into neighbouring cells. This must happen somewhere downstream in the dynodes chain, i.e. *post-first-dynode*, since no enough charge is drawn to emulate the 1PE signal. This hypothesis is supported by the correlation observed in Fig.2. The correlation can be translated into words as: "The more the charge is injected in the illuminated pixel, the larger the number of secondary electrons produced in the injected pixel is and therefore the larger number of leaking electrons into neighbouring pixels will be, for a constant probability of leakage".

Further studies on the EXT probability independence on the charge injected for different light levels can be found in [4].

An increase of the RMS of the EXT distribution was appreciated in the closest pixels to the injected pixel as is shown in Fig.5. The cause for this broadening is not well understood, however it can be an artifact of the 2D-cut method used. The 2D-cut is performed at 2.5σs (98.8% probability) on the pedestal width (45ADC counts). 45ADC counts also corresponds to 1.5σs (89.0% probability) of the 1PE peak[2]. Hence, there is a approximately 10% probability that the some 1PE hits may have been associated to the EXT rather to the OXT by the 2D-cut. Further support to this hypothesis lies on the fact that the broadening happens when the interpixel distance is the smallest, which is when the probability of the OXT tends to maximise.

[2]From the gains measured at Oxford, we can infer that the 1PE peak has a mean of 188ADC counts. The width is approximately 50% width for the setting of the MINOS M64s

4 Optical Crosstalk

This component causes the 1PE peak in the charge distribution of cross-talked pixels, hence its mechanism has to be *pre-first-dynode*. OXT is independent from EXT, therefore we shall subtract the shift from zero characteristic of EXT, for every measurement of OXT.

We tested whether a Poissonian distribution (Eq. 2) would accurately describe the average number of PEs drawn due to OXT (λ).

$$P(\lambda, n) = \frac{\lambda^n \exp -\lambda}{n!} \tag{2}$$

However, the average number of PEs injected ($< N_{pe} >$ or λ) due to OXT can be estimated in two different methods.

- *Method 1* uses the mean charge in OXT (in PE units) as shown in Eq.3.

$$< N_{pe} >= \frac{< Q_{OXT} > - < Q_{EXT} >}{Gain} \frac{N_{OXT}}{N_{total}} \tag{3}$$

  Where N_{OXT} and $< Q_{OXT} >$ are the number of entries and average charge of the OXT peak, correspondingly. This method requires the knowledge the gain of the cross-talked pixel: $Gain$. N_{total} is the number of entries in the original charge distributions of the cross-talked pixel before the 2D-cut, i.e. 10,000 flashes.

- *Method 2* assumes that the probability of OXT is described by a Poissonian distribution. Hence $< N_{pe} >$ is obtained from Eq. 4.

$$< N_{pe} >= -\ln P(n = 0) = -\ln \frac{N_{EXT}}{N_{total}} \tag{4}$$

  Where N_{EXT} is the number of entries in EXT.

OXT probability can be computed from the ratio of average number of PEs injected in the cross-talked pixel due to OXT $< N_{pe} >$ (by method 1 and/or by method 2) to the total number of PE measured at the anode of the illuminated pixel.

Fig. 6 shows the comparison between the OXT probability dependence upon the distance between illuminated and cross-talked pixels described by method 1 and method 2. Both methods describe well the strong dependence of the OXT upon the distance between the illuminated and cross-talked pixels. Furthermore, overall good agreement is found between the two methods. This suggest an avenue to for the implementation of OXT into MINOS detector *Monte Carlo*.

A non-statistical 10% discrepancy is found for the interpixel distance equals to 1. The cause for such a difference is not well understood, but may be related to limitations of the 2D-cut. This discrepancy sets the limit of accuracy of our Poissonian description of OXT. All error bars shown in this note are statistical, no further studies on systematic arising from the limitation of this 2D-cut method were explored during the course of this studies.

An interesting test on the nature of OXT arises from the fact that if the OXT was dominated by the actual 1PE peak distribution, one could extract information about the gain of the cross-talked pixel from the mean charge injected due to crosstalk as seen in Eq. 5.

$$Gain_{Crosstalk} = \frac{< Q_{total} > - < Q_{EXT} >}{\lambda} \tag{5}$$

Fig. 7 shows the difference from the gain estimated from crosstalk charge distributions and the gain measured at the Oxford test stand in dedicated runs. The overall offset of 19ADC (10% of 1PE) can be considered as a succesful confirmation that the OXT is dominated by the 1PE peak. The fact that the offset is systematically negative hints for an underestimation of the gain when using crosstalk distributions. Note that this 10% is consistent with a 10% offset between the two methods to estimate the λ for the closest pixels OXT found Fig. 6. For this comparison, there has been no account for the gain drift with temperature, however this effect is expected to be approximately 0.5% per degree C and the temperature was kept constant within at most 3 degrees C during data taken.

Two mechanisms are consistent with a *pre-first-dynode-caused* crosstalk. None of them are strongly supported by the data with the analysis method used.

- *Mechanism 1*: the 1PE get collected by a neighbouring pixel after photo-conversion.
- *Mechanism 2*: the photon scatters in the glass prior to the photo-cathode causing eventually the PE somewhere else in another pixels collection region.

OXT shows also some asymmetries in the amount of cross-talked exhibited in the closest non-diagonal cross-talked pixels, as shown by Fig.8. This may be consistent with systematic misalignment of the *"cookie"* with respect to the pixel of the PMT[3] or that OXT reflects the geometrical structure of the first dynodes of the PMT (which may favour the mechanism 2), as shown in Fig.9. No obvious way for discrimination between the two was found during this analysis.

5 Conclusions

Crosstalk in the M64 PMTs has been identified and measured. We found that the crosstalk of the M64s is dominated by two components. A 2D-cut was developed to separate both contributions since their origins were thought to be different.

The first component called *Electrical Crosstalk* causes the the whole distribution to shift toward positive charge values. It can be measured from the position of the shifted pedestal. Its origin must be post-first-dynode, whose charge is therefore less than 1PE charge equivalent. Our hypothesis for the mechanism behind is the leakage of the secondary electrons from the injected to the cross-talked pixels as electrons travel toward the anodes. This component of crosstalk should not be visible at the MINOS detectors after sparsification of the pedestal peak.

[3]Note that this effect should be systematic for all the PMTs tested.

The second component was called *Optical Crosstalk*. It is characterised by the occurrence of PE peaks in the charge spectrum of the cross-talked pixels. The amount of cross-talked charge is high enough to be above sparsification and therefore it will be seen in MINOS. Its probability seems to be well characterised by a Poissonian distributions to a 10% accuracy.

The amount of crosstalk in the M64 for both components exhibits, as expected, a strong dependence upon the distance between the non-injected and injected pixels.

References

[1] Hamamatsu Photonics K.K., "Photomultipliers Tubes - Basics and Applications", (1999).

[2] The MINOS Collaboration, *The MINOS Detectors Technical Design Report*, NuMI-L-337 (1998).

[3] M. Barker, A. De Santo, A. Weber, "Results from 'production' test of 13 R5900-00-M64 photo-tubes", NuMI-L-682 (2000).

[4] A. Cabrera*et al.*, "Hamamatsu R5900-00-M64 Characteristics Measured by the Oxford Test Stand", NuMI-934 (2003).

[5] S. Eilerts *et al.*, "Evaluation of Hamamatsu M64 for use in the near MINOS detector", NuMI-L-568 (2000).

[6] Alfons Weber, Karol Lang, Jenny Thomas, "Request for Quotation and Technical Specifications for R5900-00-M64 PMTs for the MINOS Near Detector", NuMI-L-720 (2001).

[7] Hamamatsu Photonics K.K., "R5900-00-M64 PMT Data Sheet", (2000).

[8] W.R.Leo, "Techniques for Nuclear and Particle Physics Experiments", (Springer - 1994).

[9] Glenn F Knoll, "Radiation Detection and Measurements", (John Wiley & Sons - 1999).

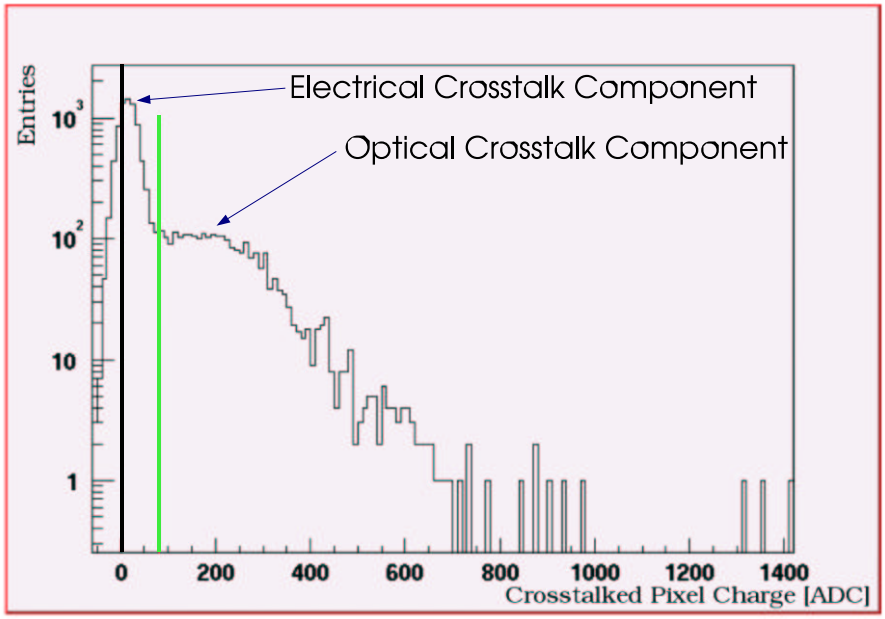

Figure 1: *Charge Spectrum of a Cross-Talked Pixel.* The black line emphasises the position of the zero charge, after pedestal subtraction. The green line is the 1D projection of the 2D-cut used to separate the two crosstalk components found in M64s. EXT is the shifted pedestal distribution toward positive charge values (shown to the left of green line). Whereas OXT causes the 1PE dominated peak (shown to the right of the green line).

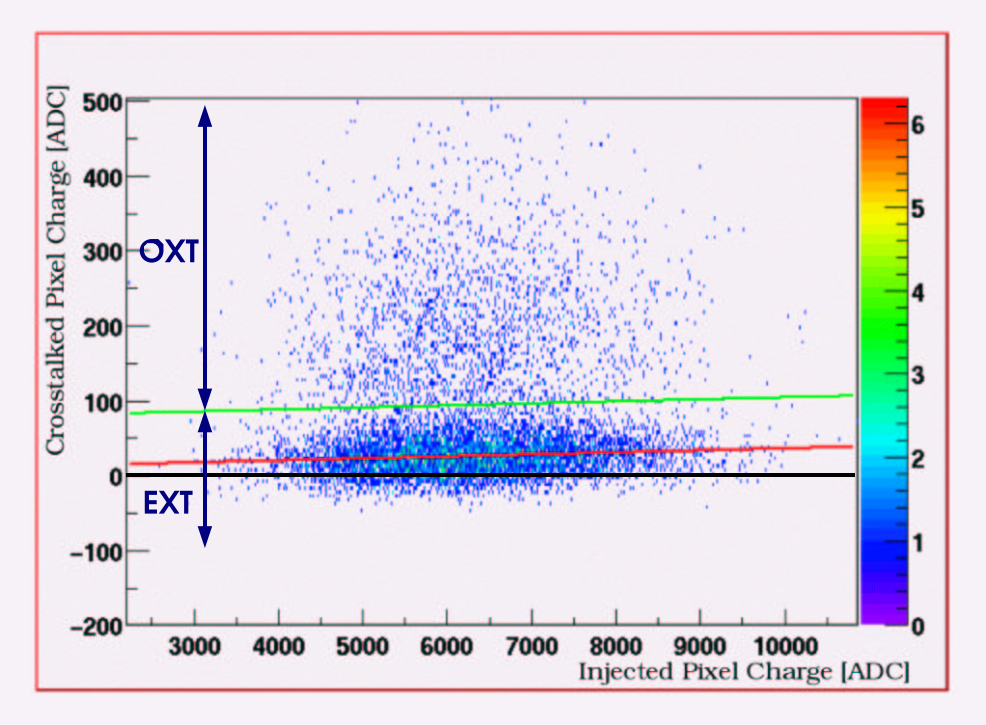

Figure 2: *Charge Spectra of an Injected Pixel versus Charge Spectra of one Cross-Talked Pixel.* Correlation between the two spectra can be clearly seen. The red line is a fitted strait line to the EXT distribution used to measure the slope of the correlation. The information from the fit is fed into definition of a 2D-cut to separate both OXT (above the green line)and EXT (below the green line). The 2D-cut is illustrated by the green line.

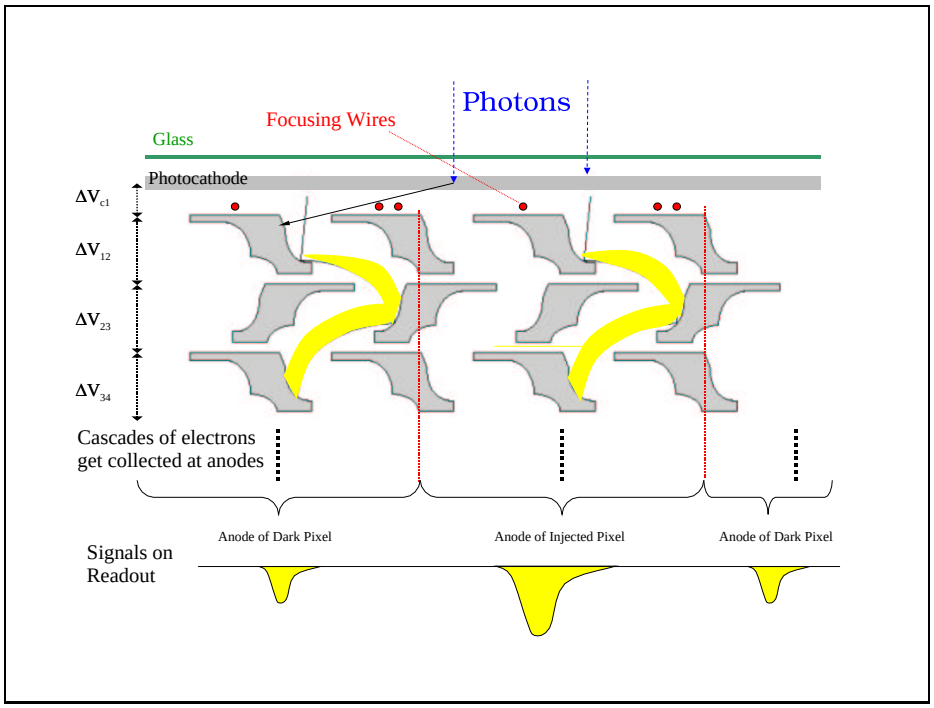

Figure 3: *Cartoon of Crosstalk in the M64.* This drawing intends to guide intuition on how crosstalk of the M64 works. The OXT occurs by a PE creating a cascade of secondary electrons in a non-illuminated pixel, while EXT happens somewhat downstream in the dynode chain due to the leaking of secondary electrons into neighbouring pixels.

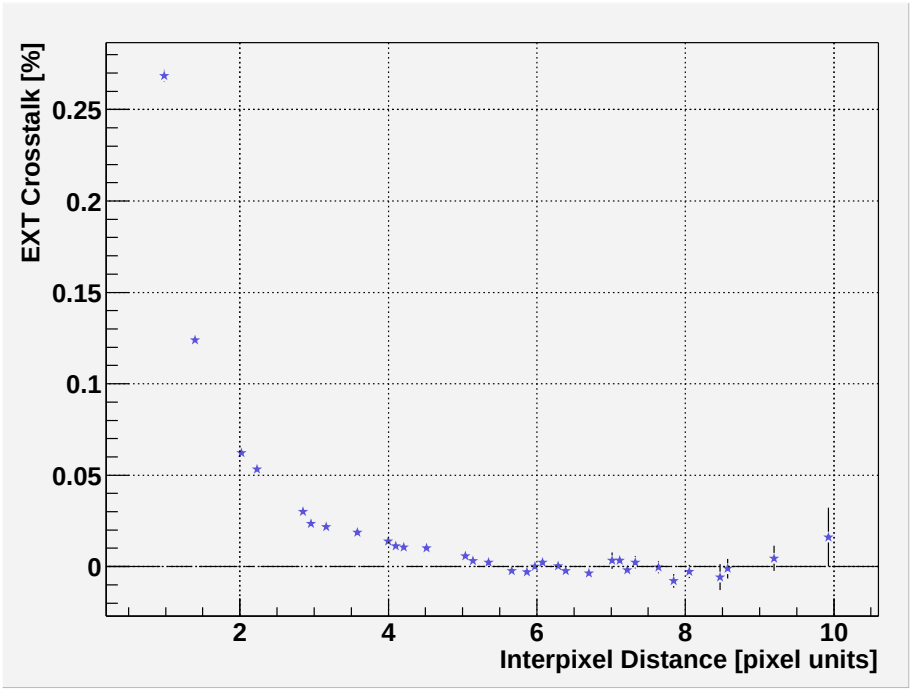

Figure 4: *Dependence of Electrical Crosstalk upon the Distance between Injected and Cross-Talked Pixels.*Up to approximately 0.1PEs can be drawn by EXT.

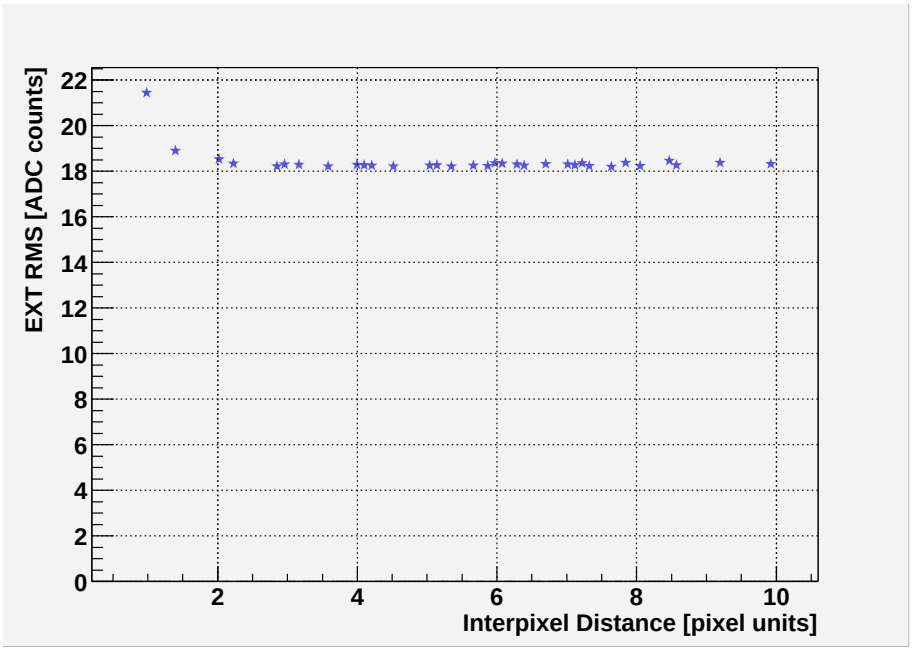

Figure 5: *Broadening of the EXT Distribution.* The EXT distribution tends to get wider in the closest pixels to the injected pixel.

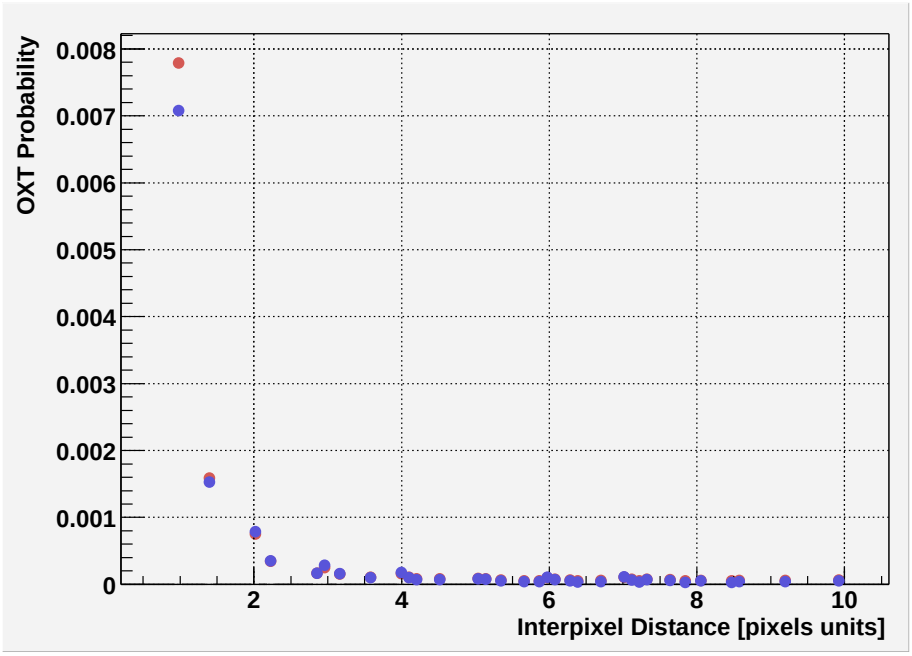

Figure 6: *Characterisation Model for OXT.* Two models are used to measure the probability of OXT as a function of the distance between the cross-talked and the injected pixel. The blue curve shows the *Method 1* in which OXT probability is calculated from the mean charge in the OXT distribution. Whereas in red curve shows the *Method 2* uses a Poissonian distribution to estimate the average number of PEs caused by OXT. There is general agreement in the pattern between the two methods, however 10% disagreement remains at the closest non-diagonal pixels from the estimation of the average number of PEs due to OXT.

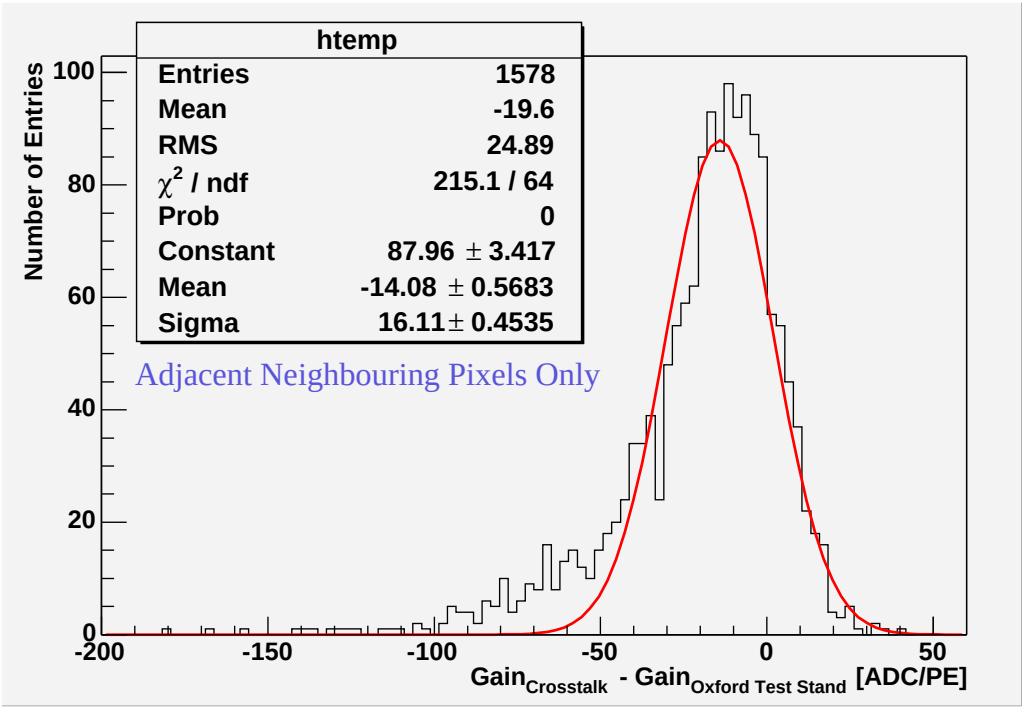

Figure 7: *Difference between the gain estimated from the charge distribution cross-talked pixels and the dedicated measurements of the gain made at Oxford test stand.* The fact that the OXT distribution is dominated by the occurrence of PE peaks with a very low mean allows sensitivity for a gain estimate for the cross-talked pixels. The comparing the crosstalk gain estimate with dedicated measurements taken at Oxford test stand reveal good agreement between the two methods. A systematic offset of about 10% of a PE may show that measurements coming from crosstalk may be underestimating the gain.

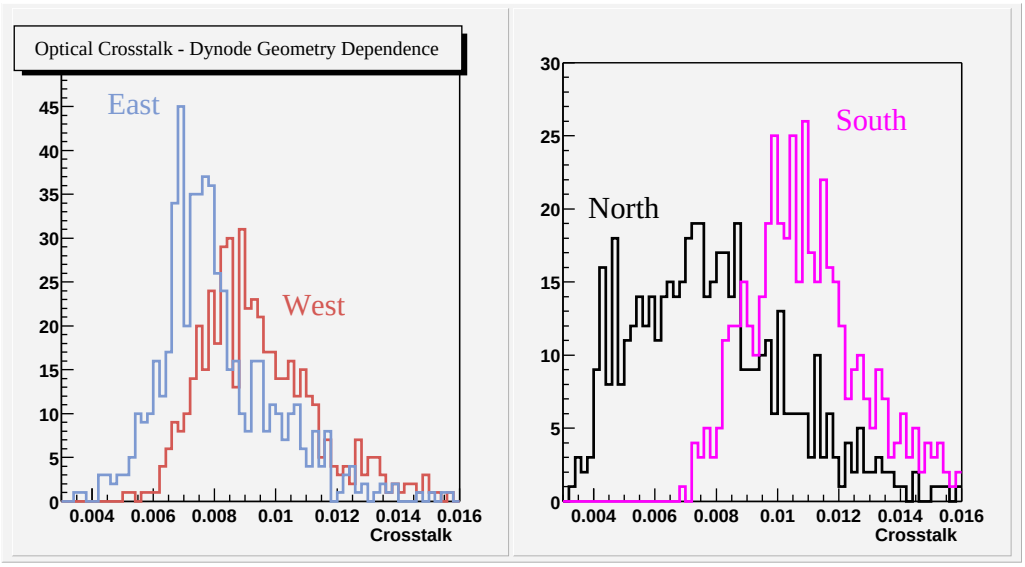

Figure 8: *OXT Dependence upon the Position of the Cross-Talked Pixel.* The cause of the asymmetry is not well understood. A systematic misalignment as well as the reflection by OXT of the structure of the first dynode in the M64 could be possible explanations.

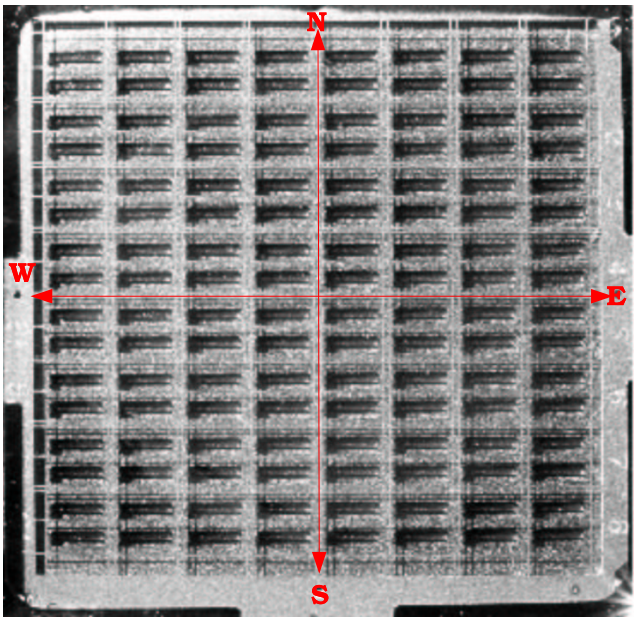

Figure 9: *First Dynode Geometrical Structure.* This plot shows the geometrical structure of the first dynodes of the M64. Collection efficiency may reflect the asymmetries of such an structure. We considered using this handle to discriminate between different mechanisms of OXT. However other potential effects like misalignment could fake the pattern expected. (Courtesy of the Oxford University Photographic Unit)